REPORT DOCUMENTATION PAGE

AFRL-SR-AR-TR-04-

0319

1. REPORT DATE (DD-MM-YYYY)	2. REPORT TYPE	3. DATES COVERED (From - To)
16-06-2004	Final Report 2004	2/1/01-2/29/04

4. TITLE AND SUBTITLE
Nanocrystal Ceramics

5a. CONTRACT NUMBER

5b. GRANT NUMBER
F49620-01-1-0033

5c. PROGRAM ELEMENT NUMBER

6. AUTHOR(S)
A. Paul Alivisatos

5d. PROJECT NUMBER

5e. TASK NUMBER

5f. WORK UNIT NUMBER

7. PERFORMING ORGANIZATION NAME(S) AND ADDRESS(ES)

University of California,
Berkeley
Department of Chemistry
D43 Hildebrand Hall
Berkeley, CA 94720-1460

8. PERFORMING ORGANIZATION REPORT NUMBER

9. SPONSORING / MONITORING AGENCY NAME(S) AND ADDRESS(ES)
AFOSR/NL
4015 Wilson Blvd., Rm 713
Arlington, VA 22203-1954

10. SPONSOR/MONITOR'S ACRONYM(S)
AFOSR/NL

11. SPONSOR/MONITOR'S REPORT NUMBER(S)

12. DISTRIBUTION / AVAILABILITY STATEMENT

Approve for Public Release: Distribution Unlimited.

20040625 126

13. SUPPLEMENTARY NOTES

14. ABSTRACT

We have two major findings, as well as more incremental progress in other areas. We have discovered a new and very general method for forming hollow oxide nanocrystals, and for encapsulating other materials inside these hollow crystals. We have demonstrated that there is a critical length for a nanorod, below which it can reversibly undergo a solid-solid phase transition with volume change, while above this length the rods fracture. Finally, we have made progress in the shape control of titanium dioxide nanocrystals, and we have improved our understanding and control over the nucleation of iron oxide nanocrystals. We have also initiated a new program to study nanocrystals at very high laser excitation energies, and we have continued our studies of nanorod liquid crystals.

15. SUBJECT TERMS
Nanocrystals, hollow oxide nanocrystals, liquid crystals of nanorods

16. SECURITY CLASSIFICATION OF:			17. LIMITATION OF ABSTRACT	18. NUMBER OF PAGES	19a. NAME OF RESPONSIBLE PERSON
a. REPORT	b. ABSTRACT	c. THIS PAGE			A. Paul Alivisatos
Unclassified	Unclassified	Unclassified			19b. TELEPHONE NUMBER (include area code) 510-643-7371

Final Technical Report
Nanocrystal Ceramics
AFOSR Grant No. F49620-01-1-0033
2/1/01 – 2/29/04

A. Paul Alivisatos
Chancellor's Professor of Chemistry and Materials Science

Department of Chemistry
University of California, Berkeley
Berkeley, California 94720-1460

T 510 643 7371
F 510 642 6911
Email: alivis@uclink4.berkeley.edu

Objectives:

- Ceramic and oxide nanocrystals will be prepared and isolated
- Nanocrystals will be characterized structurally
- Kinetic studies of reaction and phase transition processes in oxide nanocrystals

Status of effort:

We have two major findings, as well as more incremental progress in other areas. We have discovered a new and very general method for forming hollow oxide nanocrystals, and for encapsulating other materials inside these hollow crystals. We have demonstrated that there is a critical length for a nanorod, below which it can reversibly undergo a solid-solid phase transition with volume change, while above this length the rods fracture. Finally, we have made progress in the shape control of titanium dioxide nanocrystals, and we have improved our understanding and control over the nucleation of iron oxide nanocrystals. We have also initiated a new program to study nanocrystals at very high laser excitation energies, and we have continued our studies of nanorod liquid crystals.

Accomplishments/New Findings:

1. Hollow oxide nanocrystals.

We have discovered that it is possible to systematically prepare hollow oxide nanocrystals by starting with a metallic particle and oxidizing it slowly. The metal atoms diffuse outwards from the core during the oxidation, resulting in the hollow structure. This is an example of the "nanoscale Kirkendall effect." The Kirkendall Effect states that, if there is a net flow of matter in the reaction between two adjacent solids, then there will be an equal and opposite net flow of vacancies, which condense to form pores. Our work shows that in nanocrystals, this will lead to hollow structures.

In collaboration with Professor Gabor Somorjai, we have also shown that we can incorporate Pt nanocrystals inside a hollow cobalt oxide shell. Further, the shell transmits gases, so that the whole system can act as a catalytic reactor. This work was recently published in the journal *Science.*

2. Critical size for fracture in nanorods

We have shown that CdSe nanorods can be transformed from the 4 coordinate wurtzite structure to the six-coordinate rocksalt structure with 18% volume reduction under pressure. For nanocrystals of 4 nm diameter, and length less than 10 nm, we find that the nanocrystals can undergo this transformation reversibly over multiple cycles. For nanocrystals longer than 10nm, the nanorods fracture during the transformation. Further,

the fracture leads to at least three fragments. This work has been published in Nano Letters and has been transmitted in preprint and PowerPoint form to the program officer.

3. Shape control of titanium dioxide nanocrystals

We have shown that we can widely control the shapes of titanium dioxide nanocrystals by adjusting the surfactants present during the nanocrystal growth. We prepared bullet shaped nanocrystals, rods, and branched structures. Many of the features of the shape control follow predicted patterns based on other related systems, so that a more general view of how to control shapes is emerging. This work was published in the *Journal of the American Chemical Society.*

4. Synthesis of iron oxide nanocrystals

We demonstrated a new concept for control of nanocrystal growth, called "delayed nucleation." In this approach, a precursor is injected into hot surfactant solution, but the precursor must undergo a significant, and slow chemical rearrangement prior to formation of the "monomer" that yields the nanocrystal growth. This "monomer" population builds up slowly, but since the rate of nucleation depends exponentially on concentration, the moment the monomer concentration exceeds a critical value, nucleation begins. The onset of nucleation now lowers the monomer concentration, so that the time over which nucleation can occur is very brief. This method of nucleation control is advantageous as it is highly reproducible. This work is in preparation for publication.

5. Liquid crystals of nanorods.

We have continued to study the phase diagrams of nanorod liquid crystals. We have found that the phase diagram of 4x40 nm nanorods of CdSe differ from the predictions of hard rod theory, indicating substantial attractive forces between the rods. This work was published in the *Journal of Chemical Physics*.

6. Photo-ionization of colloidal nanocrystal quantum dots at high laser intensities.

Multielectron ionization of colloidal CdSe quantum dots under intense femtosecond UV excitation has been studied. By directly probing the absorption from the ionized electron, quantitative measurements of the yield and dynamics of the ionization have been made as a function of excitation influence and variations of size and potential structure of quantum dots. As many as 30 electrons can be ejected from a 3.5 nm diameter colloidal quantum dot, transiently producing a highly charged species The results have been explained by ionization mechanism involving resonant two-photon absorption. This work was published in *Physical Review Letters*.

Comprehensive Technical Summary:

Our most significant finding, formation of hollow nanocrystals through the Nanoscale Kirkendall Effect, is described in detail below:

Porous solid materials are important in many areas of modern science and technology, including ion exchange, molecular separation, catalysis, chromatography, microelectronics, and energy storage (1-3). Notable examples are microporous (< 2 nm) zeolites and mesoporous (2-50 nm) silicate and carbonaceous materials. The ability to manipulate the structure and morphology of porous solids on a nanometer scale would enable greater control of local chemical environment (4-6). We demonstrate that nanoscale pores can develop inside nanocrystals with a mechanism analogous to void formation in the Kirkendall Effect, where the mutual diffusion rates of two components in a diffusion couple differ by a considerable amount (7). We choose cobalt nanocrystals as a starting material to show that hollow nanocrystals of cobalt oxide and chalcogenides can be successfully synthesized by reacting cobalt colloidal solution with oxygen, and sulfur or selenium.

It has been known for over half a century that porosity may result from differential solid-state diffusion rates of the reactants in an alloying or oxidation reaction. In 1947, Smigelkas and Kirkendall reported the movement of the interface between a diffusion couple, i.e., copper and zinc in brass, as the result of the different diffusion rates of these two species at an elevated temperature (7). This phenomenon, now called the Kirkendall Effect, was the first experimental proof that atomic diffusion occurs through vacancy exchange, and not by the direct interchange of atoms. The net directional flow of matter is balanced by an opposite flow of vacancies, which can condense into pores or annihilate at dislocations. Directional material flows also result from coupled reaction-diffusion phenomena at a solid/gas or solid/liquid interface, leading to deformation and/or void formation during the growth of metal oxide or sulfide films (8, 9). These voids are usually explained by outward transport of fast-moving cations through the oxide layer and a balancing inward flow of vacancies to the vicinity of the metal-oxide interface. Interface motion and the formation of pores have been studied due to their impact on the reproducibility and reliability of solders, passivation layers, diffusion barriers etc., but not generally as a method of preparing porous materials. The pores produced at a metal-metal diffusion couple or near the metal-oxide interface of a growing oxide do not yield monodisperse, ordered arrays but form a very heterogeneous ensemble. Also, the observed volume fraction for pores is commonly much smaller than would be expected for the known material flows. These observations are a direct result of the large volume of material that vacancies can diffuse into and the large number of defects they can react with (10).

If the faster-diffusing species is confined into a nanocrystal 'core', the net rate of vacancy injection should increase dramatically due to the high surface-to-volume ratio of the particle and the absence of defects in the core. Within the small volume of a transforming nanocrystal, the supersaturated vacancy cloud is likely to coalesce into a single void. Previous studies on the interdiffusion of 30-micrometer powders with

layered composition showed significant porosity, but the geometry and distribution of the pores were not uniform, probably due to aggregation and bulk-like dimension of the particles (11). Significant progress has recently been made in synthesizing colloidal nanocrystals with well-controlled size, shape and surface properties (12-14). Employing such high-quality nanocrystals as the starting materials, it should be possible to produce a relatively uniform population of hollow nanostructures.

We have chosen cobalt nanocrystals as the main starting material. A number of chemical methods have been developed to synthesize uniform cobalt nanocrystals in solution (12, 15). Furthermore, cobalt reacts readily with other species such as sulfur and oxygen. Since cobalt is the major component in one class of superalloys, its high-temperature oxidation and sulfidation have been well studied (16, 17). It is known that oxidation and sulfidation of bulk cobalt under vapor at high temperature is mainly controlled by outward diffusion of cobalt cations (18). This mode of growth operating on nanocrystals is expected to lead to hollow structures.

Sulfidation of cobalt was the first case where we observed hollow nanostructures. Cobalt sulfide hollow nanospheres are synthesized in one pot by immediate injection of a solution of sulfur in *o*-dichlorobenzene into a hot cobalt nanocrystal dispersion (as shown in the transmission electron microscopy (TEM) image in Fig. 1A) that is prepared by literature methods (15, 19). At 445 K, the reaction between cobalt and sulfur completes within a few seconds, resulting in a black solution of cobalt sulfide nanocrystals. We have confirmed that hollow particles are produced at temperatures as low as 373 K. The hollow particles are very stable in solution suggesting that the chemical transformation of the surface does not disrupt the coating of the nanocrystals by surfactant molecules. Upon washing with methanol, the surfactant layer is removed and it is no longer possible to redissolve the precipitate in *o*-dichlorobenzene.

Outward flow of cobalt through the sulfide shell results in supersaturation of vacancies, which condense to form a single hole in each nanoparticle (Figs. 1B-D). Two stable cobalt sulfide phases are observed, linnaeite (Co_3S_4) and cobalt pentlandite (Co_9S_8), depending on the sulfur-to-cobalt molar ratio used in the synthesis. X-ray powder diffraction (XRD) patterns in Fig. 1E show the evolution of the crystal structure as the molar ratio of sulfur to cobalt is increased. Co_9S_8 is the only sulfide phase observed when the molar ratio is lower than 9:8, while Co_3S_4 also appears in the patterns when the molar ratio slightly exceeds this value. Only Co_3S_4 is obtained when the molar ratio of sulfur to cobalt is above 3:4. The size distribution of the sulfide hollow particles is similar to the starting cobalt nanocrystals. Monodisperse hollow nanocrystals self-assemble into ordered hexagonal arrangements when evaporated slowly on the surface of a carbon coated TEM grid. The assembly process is driven by surface tension and van der Waals forces. Cobalt sulfide nanocrystals do not form superlattices as readily as cobalt nanocrystals do, probably due to a diminished van der Waals force (19). Assemblies of hollow nanoparticles present a distinct topology of ordered porous materials. In terms of the accessibility of pores from the outside, they fall between mesoporous materials with accessible channels and void lattices where pores are confined in a continuous matrix (20).

Kinematical diffraction simulations (fig. S1) indicate that the XRD peaks are too broad to be consistent with a single crystal shell of dimensions observed by TEM (21). Satisfactory fits to the data in Figs. 1E(d) and 1E(g) are obtained by assuming ~ 4 nm cubic crystalline domains. The fits also provide a confirmation of our phase assignments. TEM micrographs (Fig. 1D) of the same sample show that the average outer diameter of the hollow Co_9S_8 nanocrystals is around 15 nm. A reasonable explanation is that the shell of each hollow sphere is multi-crystalline. This is confirmed by high resolution transmission electron microscopy (HRTEM), which shows that both Co_9S_8 and Co_3S_4 hollow nanocrystals are composed of multiple crystallographic domains (Fig. 1C). The arrangement of the domains is analogous to the columnar morphology of grains often observed in thin film growth. The multi-crystalline structure implies possible applications of these hollow nanocrystals as nanoscale reactors since small molecules may be able to penetrate the shell through the grain boundaries.

In all instances of sulfidation, we have found that the diameter of the hole in the center of the nanocrystals is 40-70% of the initial particle size (starting with cobalt particles with a size distribution of 7%, a single synthesis yields a hole size distribution of 13%). If sulfur transport through the growing shell is negligible, as shown for bulk sulfidation by marker experiments (18), then the two diameters are expected to be identical. Significant inward sulfur transport could occur through grain boundaries or during the formation of the first few monolayers of sulfide. It is also possible that inward relaxation of the hole occurs, due to annihilation of vacancies at a semicoherent or incoherent cobalt-sulfide interface. Finally, the estimation of the hole size by visual inspection of TEM images may produce systematic errors. We attempted to examine the possibility of inward sulfur transport by performing the Co_3S_4 synthesis at different sulfur concentrations. Increased sulfur concentration increases hole size and enhances outward growth of the shell, indicating that cobalt mobility rather than sulfur mobility is affected. This finding is consistent with bulk sulfidation studies (18), where it is observed that an increased sulfur vapor pressure leads to injection of more cation vacancies into the growing sulfide and enhances the parabolic rate constant for sulfide growth.

For bulk cobalt, the rates of oxidation are 3-4 orders of magnitude lower than those of sulfidation above 750 K (18). This is also true under the conditions we use to produce hollow nanocrystals, and oxidation of nanocrystals takes about three hours at 455 K. Fig. 2(A-D) shows the evolution of the morphology of the nanocrystals with time as an O_2/Ar mixture is flowed through the cobalt colloidal solution. The XRD shows the presence of metallic cobalt up to 30 minutes (Fig. 2E). The solution of particles still displays weak ferrofluidic response to a 1T magnet at that point, suggesting that small cobalt cores remain. It takes about three hours for the cobalt cores to be completely consumed: central pores are clearly distinguishable for all nanocrystals under TEM and the solution shows no magnetic response. XRD simulations (fig. S1) suggest a multicrystalline structure with a crystal domain size of ~3 nm, in agreement with HRTEM observations (Fig. 2 inset).

The evolution of hollow morphology is best illustrated by following the reaction of cobalt nanocrystals with selenium. In bulk systems, annihilation of excess vacancies at dislocations and boundaries can produce stresses leading to the formation of cracks

near the interface; the cracks then act as nuclei for the further condensation of supersaturated vacancies (11). While the exact mechanism is likely to be different, in nanocrystals voids also begin to develop and merge at the boundary (Fig. 3). The high defect content and surface energy associated with the boundary favors the nucleation of voids there. Also, as vacancies diffuse inwards, they will be more concentrated at the boundary rather than in the interior of the core. As the reaction proceeds in time, more cobalt atoms diffuse out to the shell and the accompanying transport of vacancies leads to growth and merging of the initial voids. This results in the formation of bridges of material between the core and the shell that persist until the core is completely consumed. These bridges provide a fast transport path for outward diffusion of cobalt atoms which can then spread on the inner shell surface. A similar phenomenon was observed for bulk powders (11). We note that the growth rate of pores drops dramatically when the cobalt cores become relatively small. Most of the pore volume seems to form during the first few minutes, while it takes about 30 minutes for the cobalt cores to completely disappear. This may be due to the fact that as the bridges are also consumed during the reaction, a smaller cross-sectional area is available for solid-state transport of materials.

As an illustration of the generality of the ideas presented here, we have synthesized several other hollow nanostructures. Sulfidation of disk-shaped cobalt nanocrystals (21) was observed to result in the formation of hollow nanodisks with cylindrical pores, indicating that spherical symmetry is not required for obtaining shells of regular thickness. Preliminary studies on oxidation of iron nanospheres and sulfidation of cadmium nanospheres also resulted in hollow structures, thus validating our approach for metallic cores in general. Theoretically, the mobilities of the reacting species do not have to be drastically different to result in vacancy transport. Placing solid nanocrystals containing one reactant in a comparatively dilute solution creates an additional asymmetry that may favor the creation of hollow structures: the relatively large change in the concentration of the core material between the core and the solution provides a greater driving force for the outward diffusion of the core material. Thus, numerous combinations of reactants may be expected to produce various hollow nanostructures of insulators, semiconductors and even metals. A recent report on the formation of gold nanoboxes may involve the same mechanism at some stage, although the dimension of the structures produced is an order of magnitude larger (22).

Hollow nanocrystals offer exciting possibilities in material design for applications in catalysis, nanoelectronics, nano-optics, drug delivery systems, and as building blocks for light-weight structural materials (23-25). For example, accurate fixation of the catalyst within the pores, combined with other emerging techniques of chemical control (26), could result in better reaction control and new products. To demonstrate the use of hollow nanocrystals in catalysis, we study their function as nanoreactors each containing one noble metal nanocrystal. A Pt@CoO yolk-shell nanostructure is synthesized, in which a platinum nanocrystal of a few nanometers is encapsulated in a CoO shell. Three steps are involved in the preparation of these nanoreactors: synthesis of platinum seeds by a modified "polyol" process (27), deposition of cobalt on platinum to form Pt@Co core-shell nanocrystals, and transformation of cobalt into CoO hollow structures (28). Fig. 4A shows a typical sample of platinum particles with an average diameter around 3 nm. The deposition of cobalt onto platinum at the reaction temperature yields no alloy,

only Pt core/Co shell particles, as confirmed by XRD analyses. The oxidation reaction removes cobalt atoms away from the platinum particle surface, leading to the formation of a Pt yolk/CoO shell structure (Fig. 4B). No free platinum particles were found by TEM inspection of the Pt@CoO sample. The size of Pt@CoO particles can be controlled by changing the diameter and number of the platinum seeds, and the amount of cobalt carbonyl precursor.

In order to determine if the Pt@CoO materials were active as heterogeneous catalysts, the hydrogenation of ethylene was chosen as a model reaction since it readily occurs at ambient conditions on many transition metal catalysts. Platinum is one of the most active metals for this reaction while the activity of metallic cobalt is approximately two orders of magnitude lower (29). We found that pure CoO hollow nanocrystals are inactive for ethylene hydrogenation (30), even following a 1 h H_2 pre-reduction at 373 K. Only upon reduction at 473 K for 1 h is ethane detected at temperatures >300 K. Samples containing platinum without pretreatment are active for C_2H_4 hydrogenation at temperatures as low as 208 K. The steady state turnover frequency for ethane formation at 227 K is 8.3×10^{-3} s^{-1} (31), which is comparable to the rate of 3.5×10^{-2} s^{-1} measured on a 0.04% Pt/SiO_2 catalyst (32), and 1.7×10^{-2} s^{-1} measured on pure platinum powders (0.2 - 1.6 μm). These observations indicate that the reaction is catalyzed by platinum particles, not the CoO shell. This also confirms that a route exists for ethylene and hydrogen entry into the CoO shell interior. The grain boundaries on the shell are the most probable entry points for ethylene and hydrogen diffusion into as well as ethane diffusion out of the shell. Comparing to catalysts supported on other mesoporous materials, isolation of catalyst nanoparticles within solid shells should minimize secondary reaction of the products that degrade selectivity and product distribution. Furthermore, any synergistic interactions between catalyst and support can be more efficiently utilized when each catalyst particle is in contact with a shell of the support material.

References:

1. D. Zhao, P. Yang, Q. Huo, B. F. Chmelka, G. D. Stucky, *Curr. Opin. Solid State Mater. Sci.* **3**, 111 (1998).

2. S. A. Johnson, P. J. Ollivier, T. E. Mallouk, *Science* **283**, 963 (1999).

3. A.-P. Li, F. Müller, A. Birner, K. Nielsch, U. Gösele, *Adv. Mater.* **11**, 483 (1999).

4. D. Trong On, D. Desplantier-Giscard, C. Danumah, S. Kaliaguine, *Appl. Catal.* **222**, 299 (2001).

5. M. E. Davis, *Nature* **417**, 813 (2002).

6. W. Gu, M. Warrier, V. Ramamurthy, R. G. Weiss, *J. Am. Chem. Soc.* **121**, 9467 (1999).

7. A. D. Smigelskas, E. O. Kirkendall, *Trans. AIME* **171**, 130 (1947).

8. C. E. Birchenall, *J. Electrochem. Soc.* **103**, 619 (1956).

9. J. C. Colson, M. Lambertin, P. Barret in *Proc. 7th Int. Symp. Reactivity of Solids*, J. S. Anderson, F. S. Stone, M. W. Roberts Eds. (Chapman and Hall, London, 1972), pp. 283-293.

10. G. B. Gibbs, *Oxid. Met.* **16**, 147 (1981).

11. F. Aldinger, *Acta Met.* **22**, 923 (1974).

12. C. B. Murray, C. R. Kagan, M. G. Bawendi, *Annu. Rev. Mater. Sci.* **30**, 545 (2000).

13 X. Peng et al., *Nature* **404**, 59 (2000)

14. R. Jin et al., *Nature* **425**, 487 (2003).

15. V. F. Puntes, K. M. Krishnan, A. P. Alivisatos, *Science* **291**, 2115 (2001).

16. S. Mrowec, K. Przybylski, *Oxid. Met.* **11**, 365 (1977).

17. A. Devin, *Cobalt* **30**, 19 (1966).

18. S. Mrowec, M. Danlelewski, A. Wojtowicz, *J. Mater. Sci.* **33**, 2617 (1998).

19. V. F. Puntes, K. M. Krishnan, P. Alivisatos, *Appl. Phys. Lett.* **78**, 2187 (2001).

20. N. M. Ghoniem, D. Walgraef, S. J. Zinkle, *J. Comput. Aided Mater. Des.* **8**, 1 (2001).

21. V. F. Puntes, D. Zanchet, C. K. Erdonmez, A. P. Alivisatos, *J. Am. Chem. Soc.* **124**, 12874 (2002).

22. Y. Sun, Y. Xia, *Science* **298**, 2176 (2002).

23. F. Caruso, R. A. Caruso, H. Möhwald, *Science* **282**, 1111 (1998).

24. U. S. Schwarz, S. A. Safran, *Phys. Rev. E* **62**, 6957 (2000).

25. W. S. Sanders, L. J. Gibson, *Mater. Sci. Eng. A* **352**, 150 (2003).

26. N. J. Turro, *Acc. Chem. Res.* **33**, 637 (2000).

27. N. S. Sobal, U. Ebels, H. Möhwald, M. Giersig, *J. Phys. Chem.* **107**, 7351 (2003).

28. Platinum acetylacetonate is reduced with a long-chain polyol to form uniform platinum nanoparticles in the presence of surfactants such as oleic acid, oleylamine, and trioctylphosphine. The size of the platinum particles can be tuned from 1 to 10 nm, depending on the concentration of surfactants. $Co_2(CO)_8$ is then injected into the hot solution and decomposed to form a conformal coating on platinum nanocrystals. Oxidation of the Pt@Co nanocrystals is performed a few minutes after the introduction of cobalt carbonyl by blowing a stream of O_2/Ar (1:4 in volume ratio, 120 ml/min) mixture into the colloidal solution at 455 K. The system is kept under stirring for 3 hours. A black stable colloidal dispersion in *o*-dichlorobenzene is obtained. Finally, the Pt@CoO particles are precipitated by methanol, washed with toluene and methanol three times, and dried under vacuum. Typical nitrogen adsorption/desorption measurement on the powder at 77K shows a type IV isotherm with type H2 hysteresis, with a Brunauer-Emmet-Teller (BET) surface area of 65 m^2/g and a total pore volume of 0.0676 cm^3/g.

29. G. A. Somorjai, *Introduction to Surface Chemistry and Catalysis*. (John Wiley and Sons, Inc., New York, 1994).

30. The hydrogenation of ethylene is studied at atmospheric pressure in a differentially operated plug flow reactor. Standard conditions are 11 Torr C_2H_4, 150 Torr H_2, and 208-353K (sample dependent).

31. Rates were measured on a per gram basis. They were normalized per mole of surface platinum species (Pt_s) to obtain a turnover frequency (molecule $Pt_s^{-1}s^{-1}$). Moles of Pt_s was determined by D=1.13/d where D is the platinum dispersion (ratio of Pt_s to the total platinum content (Pt_t)) and d is the particle size in nm. The platinum particle size was determined from number average TEM measurements.

32. R. D. Cortright, S. A. Goddard, J. E. Rekoske, J. E. Dumesic, *J. Catal.* **127**, 342 (1991).

Figures

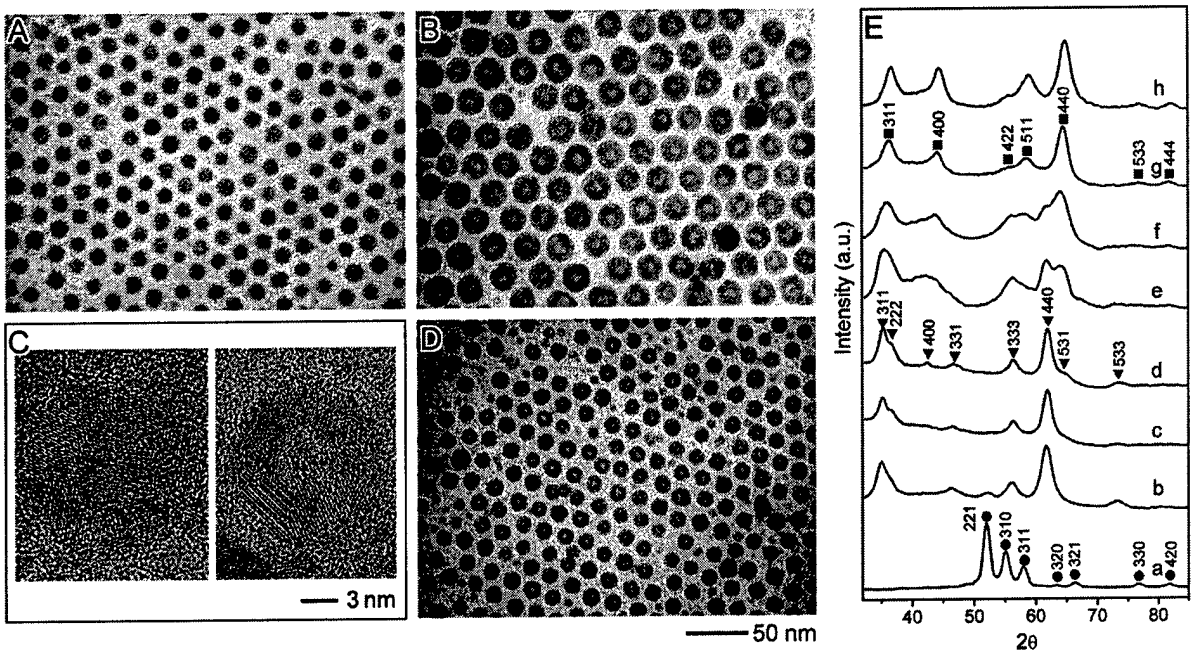

Fig. 1. (A) TEM image of cobalt nanocrystals synthesized by injecting 0.54 g of $Co_2(CO)_8$ in 3 ml of *o*-dichlorobenzene into 0.1 ml of oleic acid and 0.1 g of trioctylphosphine oxide in 15 ml of *o*-dichlorobenzene at 455 K. (B, D) TEM images of the cobalt sulfide phases synthesized by injecting sulfur in *o*-dichlorobenzene (5 ml) into cobalt nanocrystal solution with different Co/S molar ratios: (B) Co_3S_4 with Co:S=9:12 and (D) Co_9S_8 with Co:S=9:8. The Co_3S_4 particles were synthesized from the cobalt sample shown in (A), while the Co_9S_8 particles started from another cobalt sample which has an average diameter around 11 nm. (C) HRTEM images of Co_3S_4 (left) and Co_9S_8 (right). (E) XRD patterns of cobalt nanocrystals (a) and cobalt sulfide synthesized with different Co/S molar ratios: (b) 9:5; (c) 9:7; (d) 9:8; (e) 9:10; (f) 9:11; (g) 9:12; and (h) 9:18.

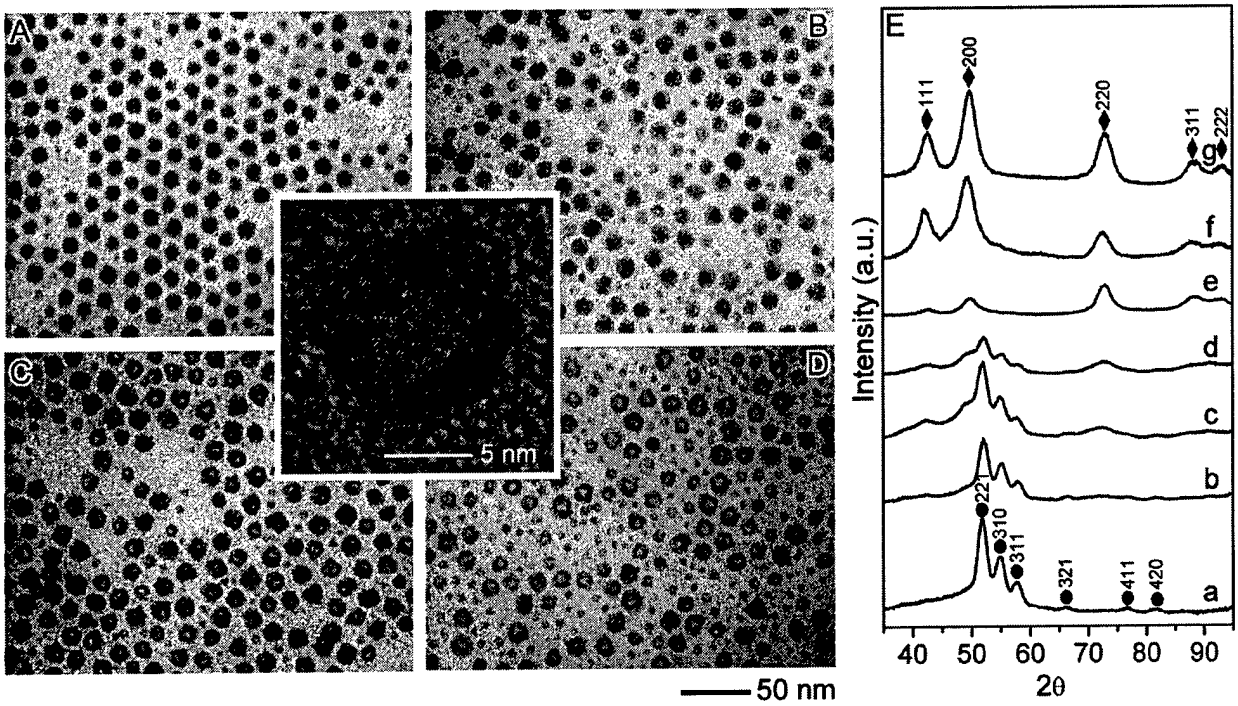

Fig. 2. Evolution of CoO hollow nanocrystals with time by blowing a stream of O_2/Ar (1:4 in volume ratio, 120 ml/min) mixture through a cobalt colloidal solution at 455 K. (A-D) TEM images of the solutions after flowing O_2/Ar for (A) 0 min; (B) 30 min; (C) 80 min; (D) 210 min. The inset shows a HRTEM of a CoO hollow nanocrystal. (E) XRD patterns of the sample obtained from the solution after flow O_2/Ar for (a) 0 min; (b) 2.5 min; (c) 5.5 min; (d) 10 min; (e) 30 min; (f) 80 min; and (g) 210 min.

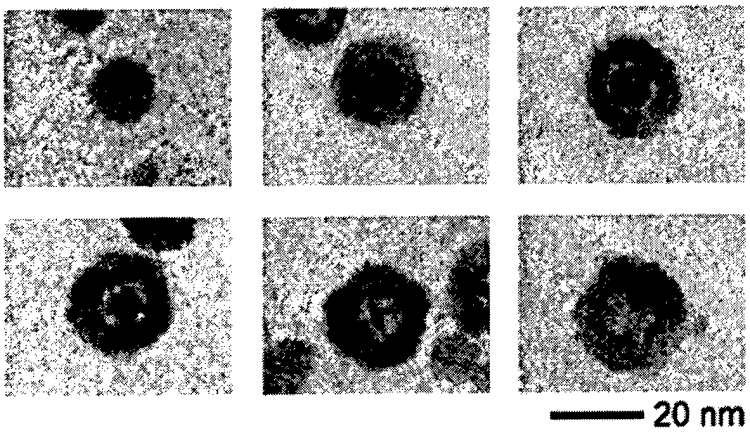

Fig. 3. Evolution of CoSe hollow nanocrystals with time by injection of a suspension of selenium in *o*-dichlorobenzene into a cobalt nanocrystal solution at 455 K, from top-left to bottom-right: 0 sec, 10 sec, 20 sec, 1 min, 2 min and 30 min. The Co/Se molar ratio is 1:1.

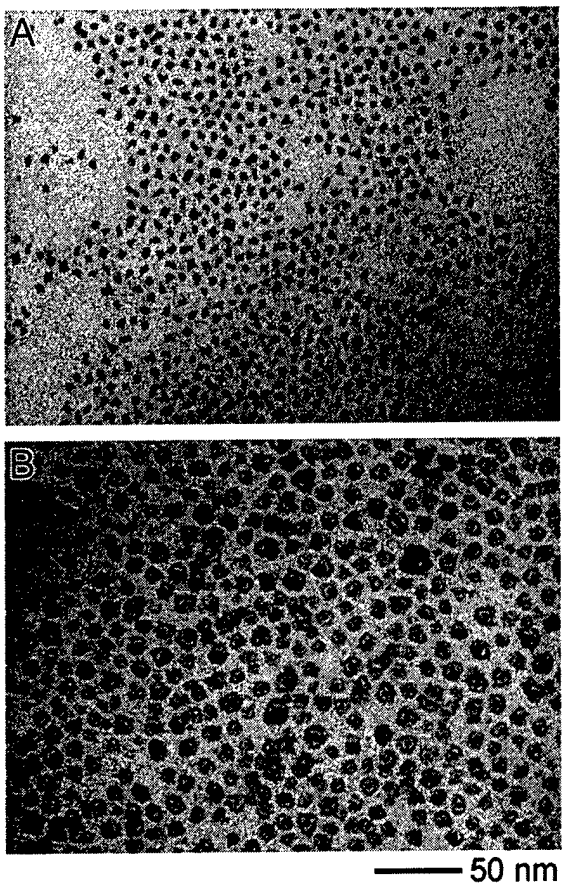

Fig. 4. (A) Platinum nanocrystals prepared by injecting a solution of 0.15 g platinum acetylacetonate in 5 ml *o*-dichlorobenzene into a refluxing bath of 10 ml *o*-dichlorobenzene containing 0.3 g of 1,2-hexadecanediol, 0.1 ml of oleic acid, 0.1 ml of oleylamine and 0.06 ml of trioctylphosphine. The solution was then heated for another 120 minutes. (B) Pt@CoO yolk-shell nanostructures formed by injecting 1.08 g $Co_2(CO)_8$ in 6 ml *o*-dichlorobenzene into the platinum nanocrystals solution, and followed by the oxidation of the product particles by blowing a stream of O_2/Ar (1:4 in volume ratio, 120 ml/min) mixture into the colloidal solution at 455 K. The system was kept at the same temperature under stirring for 3 hours.

Personnel Supported: List professional personnel (Faculty, Post-Docs, Graduate Students, etc.) supported by and/or associated with the research effort.

Principal Investigator: Paul Alivisatos
Postdoctoral Researcher: Joerg Rockenberger, Maria Francesca Casula
Graduate Student: David Zaziski
Undergraduate Student: Kevin Biggs

Publications:

David Zaziski, Stephen Prilliman, Erik Scher, Maria Casula, Juanita Wickham, Simon Clark, and A. Paul Alivisatos, "Critical Size for Fracture During Solid-Solid Phase Transformations," Nano Letters, 4, No. 5, 943-946 (April 2004).

David Zaziski, "Effects of the Solid-Solid Transformation in Nanocrystals," Ph.D. Thesis, University of California, Berkeley, Department of Chemistry, Fall 2003.

L.-S. Li, M. Marjanska, G. H. J. Park, A. Pines, and A. P. Alivisatos, "Isotropic-Liquid Crystalline Phase Diagram of A CdSe Nanorod Solution", J. Chem. Physics, 120, No. 3, 1149-1152 (January 2004).

Y-W Jun, M. F. Casula, J-H Sim, S. Y. Kim, J. Cheon, and A. P. Alivisatos, "Surfactant-Assisted Elimination of a High Energy Facet as a Means of Controlling the Shapes of TiO2 Nanocrystals", J. Am. Chem. Soc., 125, No. 51, 15981-15985 (December 2003).

K. Jacobs, D. Zaziski, E. C. Scher, A. B. Herhold and A.P. Alivisatos, "Activation Volumes for Solid-Solid Transformations in Nanocrystals," Science, 293, 1803 (September 2001).

J. Rockenberger, F. Nolting, J. Luening, J. Hu, A.P. Alivisatos, "Soft X-Ray Imaging and Spectroscopy of Single Nanocrystals," J of Chem Physics, 116, No. 14 (April 2002).

D. H. Son, J. S. Wittenberg, and A. P. Alivisatos, "Multielectron Ionization of CdSe Quantum Dots in Intense Femtosecond Ultraviolet Light," Phys. Rev. Lett., 92, No. 12, 127406-1-127406-4 (March, 2004).

New Discoveries, Inventions, or Patent Disclosures (details to be listed on "Report of Inventions" form):

A general process for forming hollow oxide nanocrystals- patent disclosure
New catalysts based on hollow oxide nanocrystals – patent disclosure
Inorganic nanorod liquid crystals – patent disclosure

Honors/Awards:

Election to the National Academy of Sciences
Election to the American Academy of Arts and Sciences
Miller's Professorship (Academic Year 2001-2002)
Chancellor's Professorship, University of California, Berkeley, 1998-2001
Fellow, American Association for the Advancement of Science
Fellow, American Physical Society